Available online at www.sciencedirect.com
SCIENCE DIRECT®
Journal of Organometallic Chemistry 681 (2003) 258–263
Journal of Organometallic Chemistry
www.elsevier.com/locate/jorganchem

Syntheses and structures of selenido dimanganese and iron–manganese carbonyl cluster complexes

Richard D. Adams *, O.-Sung Kwon, Sanghamitra Sanyal

Department of Chemistry and Biochemistry, University of South Carolina, Columbia, SC 29208, USA

Received 27 May 2003; received in revised form 17 June 2003; accepted 17 June 2003

Abstract

The bis-selenido tetramanganese complex, $Mn_4(CO)_{15}(PPh_3)_2(\mu_3\text{-}Se)_2$ (**1**), was obtained from the reaction of $Mn_2(CO)_9(NCMe)$ with $Se{=}PPh_3$. Three new bis-selenido bimetallic iron–manganese complexes, $CpFeMn_3(CO)_{13}(PPh_3)(\mu_3\text{-}Se)_2$ (**2**), $Cp_2Fe_2Mn_2(CO)_{10}(PPh_3)(\mu_3\text{-}Se)_2$ (**3**) and $Cp_2Fe_2Mn_2(CO)_{11}(\mu_3\text{-}Se)_2$ (**4**) were obtained from the reaction of $CpFeMn(CO)_7$ with $Se{=}PPh_3$ in the presence of trimethylamine N-oxide. Compounds **1**, **2** and **3** were characterized by single crystal X-ray diffraction analyses. All three complexes contain an $M_4(\mu_3\text{-}Se)_2$ cluster core with a carbonyl bridged Mn–Mn single bond.

Keywords: Iron; Manganese; Selenium; Phosphine selenide

1. Introduction

Metal carbonyl complexes containing chalcogen atoms have attracted much attention because of their high affinity for transition metal atoms [1]. Bridging sulfido ligands are often used to facilitate the synthesis of high nuclearity metal complexes [2]. Selenido ligands should also be of great value for this purpose; however, the chemistry of metal selenide complexes has been much less studied [1d,3].

Recently, we have prepared the new diselenido complex, $CpMoMn(CO)_5(\mu\text{-}Se_2)$, from the reaction of $CpMoMn(CO)_8$ with elemental selenium in the presence of Me_3NO, Eq. (1) [4]. This complex exhibits a wide range of reactivity at the diselenido ligand which includes the insertion of metal complexes and unsaturated organic molecules into the Se–Se bond.

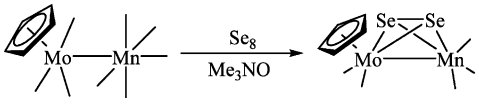

(1)

Tertiary phosphine chalcogenides R_3PE (E = S, Se, Te) have been shown to be effective reagents for the synthesis of transition metal clusters containing bridging chalcogenido ligands [5]. We have now investigated the reaction of triphenylphosphine selenide $Se{=}PPh_3$ with $Mn_2(CO)_9(NCMe)$ and with $CpFeMn(CO)_7$ activated by treatment with Me_3NO. The reaction of $Se{=}PPh_3$ with $Mn_2(CO)_9(NCMe)$ yielded the new bis-selenido tetramanganese compound $Mn_4(CO)_{15}(PPh_3)_2(\mu_3\text{-}Se)_2$ (**1**), while the reaction with $CpFeMn(CO)_7$ yielded the three new tetranuclear iron–manganese bis-selenido complexes $CpFeMn_3(CO)_{13}(PPh_3)(\mu_3\text{-}Se)_2$ (**2**), $Cp_2Fe_2Mn_2(CO)_{10}(PPh_3)(\mu_3\text{-}Se)_2$ (**3**), and $Cp_2Fe_2Mn_2(CO)_{11}(\mu_3\text{-}Se)_2$ (**4**). The molecular structures of **1**, **2** and **3** were determined by X-ray crystallographic methods. The results of these studies are reported here.

2. Results and discussion

The new bis-selenido tetramanganese compound $Mn_4(CO)_{15}(PPh_3)_2(\mu_3\text{-}Se)_2$ (**1**) was obtained in 32% yield from the reaction of $Se{=}PPh_3$ with $Mn_2(CO)_9(NCMe)$ at room temperature. Compound **1** was also characterized by a combination of IR, ^{1}H-NMR and single crystal X-ray diffraction analysis. Details of the structure of **1** were established by a single crystal X-ray diffraction analysis. An ORTEP diagram of its molecular

* Corresponding author. Tel.: +1-803-777-7187; fax: +1-803-777-6781.
E-mail address: adams@mail.chem.sc.edu (R.D. Adams).

0022-328X/03/$ - see front matter © 2003 Elsevier B.V. All rights reserved.
doi:10.1016/S0022-328X(03)00631-4

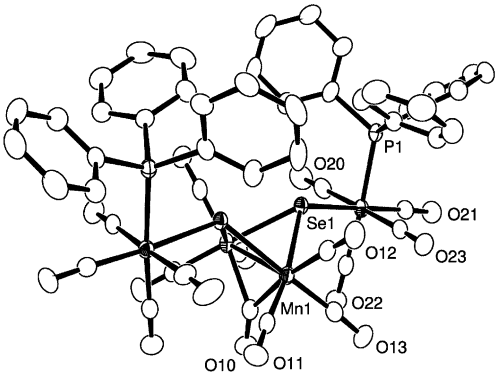

Fig. 1. An ORTEP diagram of $Mn_4(CO)_{15}(PPh_3)_2(\mu_3\text{-}Se)_2$ (**1**) showing 50% probability thermal ellipsoids.

structure is shown in Fig. 1. Selected interatomic distances and angles are listed in Table 2. The structure of **1** is structurally very similar to that of the bis-sulfido compound $Mn_4(CO)_{15}(PMe_2Ph)_2(\mu_3\text{-}S)_2$ that was obtained from the reaction of $Mn_2(CO)_7(\mu\text{-}S_2)$ with PPh_3 [6]. The molecule contains a butterfly "Mn_2Se_2" core with a bridging carbonyl ligand across the Mn–Mn bond. In the solid state compound **1** contains a crystallographically imposed two-fold rotation axis that passes through the center of Mn–Mn bond and along the CO bond of the bridging carbonyl ligand C(10)–O(10). The Mn–Mn bond length 2.6771(9) Å is slightly longer than that found in $Mn_4(CO)_{15}(PMe_2Ph)_2(\mu_3\text{-}S)_2$, 2.6356(16) Å, [6] but is very similar to that found in $Mn_2(CO)_7(\mu\text{-}S_2)$, 2.6745(5) Å which contains a sulfur–sulfur bond [6]. It is considerably shorter than the Mn–Mn distance observed in $Mn_2(CO)_{10}$, 2.8950(6) [7] and 2.9038(6) Å [8] which contains no bridging ligands. The bridging carbonyl ligand is bonded symmetrically to the two manganese atoms, Mn(1)–C(10)=Mn(1′)–C(10) = 2.083(4) Å, but the CO stretching frequency for this ligand is unusually high at 1932 cm^{-1}. This high absorption frequency is nevertheless, characteristic of the bridging CO ligands in these types of complexes and occurs at 1909 cm^{-1} for the related compound $Mn_4(CO)_{15}(PMe_2Ph)_2(\mu_3\text{-}S)_2$ [6]. Each bridging selenido ligand contains one $Mn(CO)_4(PPh_3)$ group. The Mn–Se bond distances in **1**, 2.4546(5)–2.5277(5) Å, are similar to those found in the diselenido complex $[Mn_2(Se_2)_2(CO)_6]^{2-}$, 2.474(4)–2.525(2) Å, [9] and $CpMoMn(CO)_5(\mu\text{-}Se_2)$ 2.4367(8) Å, 2.4218(7) Å and $Cp_2Mo_2Mn_2(CO)_7(\mu_3\text{-}Se)_4$, 2.3259(14)–2.5087(16) Å [4]. The bridging Mn–Se bond distances, 2.4643(5) and 2.4546(5) Å, are significantly shorter than those to the $Mn(CO)_4(PPh_3)$ group, Mn–Se = 2.5277(5) Å. The distance between two selenium atoms, Se···Se = 3.0206(6) Å, is too long to permit any significant direct Se–Se bonding.

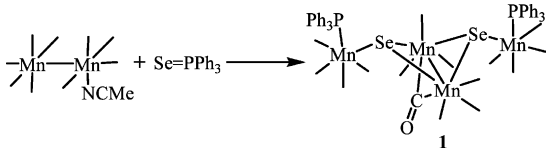

It is proposed that the reaction occurs by displacement of the labile NCMe ligand by the Se atom from the $Se{=}PPh_3$ with formation of an Mn–Se bond in an intermediate such as **A**. The Se–P bond is then cleaved and the PPh_3 may become coordinated to a manganese atom in an intermediate such as **B**. Eventually, two equivalents of the unobserved intermediate **B** dimerize to form **1**. This is probably promoted by the formation of the triply bridging selenido ligands.

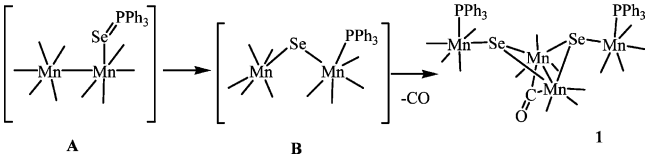

Three new selenido iron–manganese carbonyl cluster complexes: $CpFeMn_3(CO)_{13}(PPh_3)(\mu_3\text{-}Se)_2$ (**2**) (7% yield), $Cp_2Fe_2Mn_2(CO)_{10}(PPh_3)(\mu_3\text{-}Se)_2$ (**3**) (4% yield) and $Cp_2Fe_2Mn_2(CO)_{11}(\mu_3\text{-}Se)_2$ (**4**) (14% yield) were obtained from the reaction of an Me_3NO activated form of $CpFeMn(CO)_7$ with $Se{=}PPh_3$ in benzene solvent at room temperature. All three new complexes were characterized by a combination of IR, ^{1}H-NMR and mass spectral analyses. The molecular structures of **2** and **3** were also established by a single crystal X-ray diffraction analysis.

The ^{1}H-NMR spectrum of **2** exhibits a multiplet at 7.75–7.40 ppm that can be assigned to the phenyl groups of the phosphine ligand and singlet at 4.42 ppm that is assigned to the Cp ligand. Details of the molecular structure of **2** were established by a single crystal X-ray diffraction analysis, and an ORTEP diagram of its structure is shown in Fig. 2. Selected bond distances and angles are listed in Table 3. Compound **2** is structurally very similar to that of **1** except that it

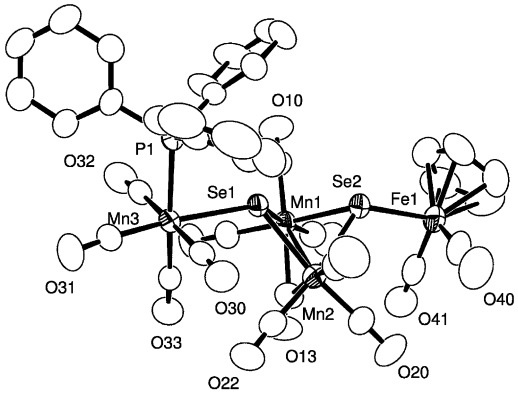

Fig. 2. An ORTEP diagram of $CpFeMn_3(CO)_{13}(PPh_3)(\mu_3\text{-}Se)_2$ (**2**) showing 50% probability thermal ellipsoids.

contains a $CpFe(CO)_2$ group terminally bonded to one of the bridging selenido ligands in place of one of the $Mn(CO)_4(PPh_3)$ groups. There is a central "Mn_2Se_2" core with a bridging carbonyl ligand across the Mn–Mn bond. The Mn–Mn bond distance, Mn(1)–Mn(2) = 2.6771(14) Å, is very similar to that observed in **1** and only slightly larger than that found in the structurally related bis-sulfido dimanganese complex $Mn_4(CO)_{15}(PMe_2Ph)_2(\mu_3\text{-}S)_2$, 2.6356(16) [6]. The Mn–Se bond distances in **2**, 2.4587(12)–2.5387(10) Å are similar to those observed in **1**, 2.4546(5)–2.5277(5) Å. The Fe–Se bond distance, Fe(1)–Se(2) = 2.4255(11) Å is similar to those found in $Cp_2Fe_4(CO)_{10}(\mu_3\text{-}Se)_2$, Fe–Se = 2.3642(8)–2.4401(8) Å, [10] and slightly longer than those found in $Fe_2(CO)_6(\mu\text{-}Se)_2$, 2.354(2)–2.378(2) Å [11a] and $Fe_2(CO)_{6-n}(PPh_3)_n(\mu\text{-}Se_2)$, [$n = 1$, 2.365(2) and 2.368(2) Å and $n = 2$, 2.370(1) and 2.389(1) Å] [11b]. The distance between two selenium atoms, Se(1)···Se(2) = 2.9970(9) Å, is too long for any significant direct Se–Se bonding interaction. The carbonyl ligand C(13)–O(13) is a symmetrical bridge within experimental error, Mn(1)–C(13) = 2.080(8) Å and Mn(2)–C(13) = 2.079(8) Å, but like **1** still absorbs at a fairly high frequency, 1927 cm^{-1} in the infrared spectrum.

An ORTEP diagram of $Cp_2Fe_2Mn_2(CO)_{10}(PPh_3)(\mu_3\text{-}Se)_2$ (**3**) is shown in Fig. 3. Selected interatomic bond distances and angles are listed in Table 3. The structure of **3** is similar to that of **1**, **2** and $Mn_4(CO)_{15}(PMe_2Ph)_2(\mu_3\text{-}S)_2$ [6], but it contains a $CpFe(CO)_2$ group terminally bonded to one of the bridging selenido ligands Se(2), and a $CpFe(CO)(PPh_3)$ group bonded to the other one Se(1). The $Mn_2(\mu\text{-}Se)_2$ core is similar to that in **1**, **2** and $Mn_4(CO)_{15}(PMe_2Ph)_2(\mu_3\text{-}S)_2$, and the Mn–Mn bond length, Mn(1)–Mn(2) = 2.6860(19) Å is also similar. The Mn–Se bond distances in **3**, 2.4517(17)–2.4929(17) Å are similar to those observed in **1** and **2**, 2.4546(5)–2.5387(10) Å. The Fe–Se bond distances, Fe(1)–Se(1) = 2.4235(16) Å and Fe(2)–Se(2) = 2.4259(18) Å, are similar to that found in **2**, Fe–Se = 2.4255(11) Å. The selenium atoms in **3** are not mutually bonded, Se(1)···Se(2) = 3.0298(13) Å. The carbonyl ligand C(13)–O(13) is an asymmetrical bridge, Mn(1)–C(13) = 2.006(11) Å and Mn(2)–C(13) = 2.128(11) Å, and absorbs at a fairly high frequency, 1933 cm^{-1} in the infrared spectrum.

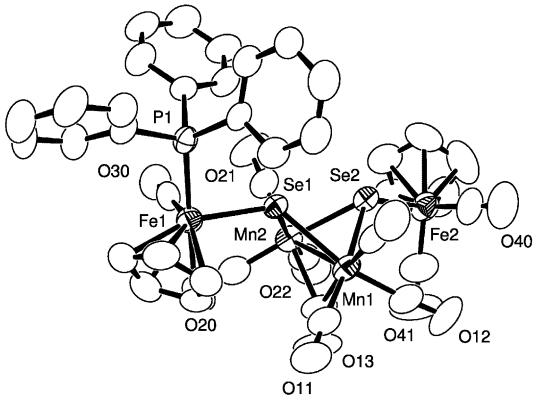

Fig. 3. An ORTEP diagram of $Cp_2Fe_2Mn_2(CO)_{10}(PPh_3)(\mu_3\text{-}Se)_2$ (**3**) showing 50% probability thermal ellipsoids.

It was not possible to obtain a single crystal of the major product **4**, but its structure can be anticipated on the basis of its mass and NMR spectral data and comparisons to those of **2** and **3**. On the basis of parent ion in the mass spectral analysis ($m/z = 821$ [M+H]), the formula of **4** was determined to be $Mn_2Fe_2Se_2C_{21}O_{11}H_{10}$. The ^{1}H-NMR spectrum at room temperature shows only one singlet at $\delta = 3.97$ ppm indicating that the two Cp ligands are equivalent. A symmetrical structure having equivalent Cp ligands on the two pendant iron carbonyl groups satisfies all this spectroscopic data. On this basis the structure shown below is proposed.

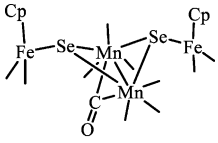

4

The reaction of $CpFeMn(CO)_7$ with $Se{=}PPh_3$ is summarized in the Scheme 1.

$CpFeMn(CO)_7$ is decarbonylated by treatment with Me_3NO. The loss of carbonyl ligand could occur at either metal atom but probably occurred on the CO-rich manganese atom. As described above for the formation of **1**, the Se atom from the $SePPh_3$ probably adds to a metal atom at this site. The Se–P bond is then cleaved and an intermediate containing one iron atom, one manganese atom and one selenido ligand is formed. The phosphine ligand could be eliminated or could coordinate to the manganese atom or the iron atom. The intermediate could then dimerize and the products **3** and **4** are formed. The formation of compound **2** could be explained by the formation of mononuclear metal fragments and scrambling of these groups among the various products.

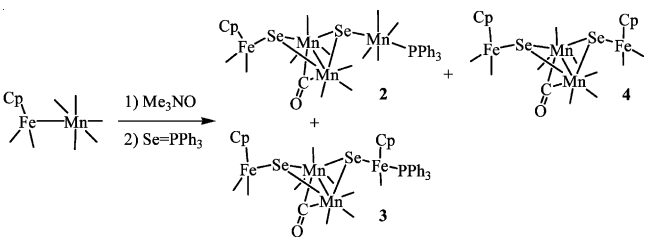

Scheme 1.

3. Experimental

3.1. General data

All reactions were performed under a nitrogen atmosphere using standard Schlenk techniques. Reagent grade solvents were dried by the standard procedures and were freshly distilled prior to use. Infrared spectra were recorded on a Nicolet Avatar FTIR spectrophotometer. ^{1}H-NMR spectra were recorded on a Varian Inova 300 spectrometer operating at 300 MHz. Mass spectra were obtained by Electrospray Ionization on a Waters Micromass Q-Tof, quadrupole time-of-flight mass spectrometer. $CpFeMn(CO)_7$ [12], $Mn_2(CO)_9(NCMe)$ [13] and $Se{=}PPh_3$ [14] were prepared according to the published procedures. Product separations were performed by TLC in air on Analtech 0.25, 0.5 and 1.0 mm silica gel 60 Å F_{254} glass plates.

3.2. Reaction of $Mn_2(CO)_9(NCMe)$ with $Se{=}PPh_3$

A 184 mg (0.457 mmol) amount of $Mn_2(CO)_9(NCMe)$ was dissolved in 50 ml toluene in a 100 ml three-neck round-bottom flask equipped with a stir bar, gas inlet and gas outlet. To this solution was added 77 mg (0.294 mmol) of $Ph_3P{=}Se$. The resulting solution was stirred for 1 h at room temperature. The volatiles were removed in vacuo and the residue was separated by thin layer chromatography over silica-gel by using hexane–CH_2Cl_2 (1/1, v/v) solvent mixture as eluant. 73.9 mg of unreacted $Mn_2(CO)_9(NCMe)$ and 96.3 mg (32% yield) of $Mn_4(CO)_{15}(PPh_3)_2(\mu_3\text{-}Se)_2$ (**1**), were obtained in order of elution. Spectral data for **1**: IR ν_{CO} (cm^{-1} in CH_2Cl_2) 2078(s), 2065(s), 2014(vs), 1963(m), 1932(s). ^{1}H-NMR (δ in $CDCl_3$), 7.58–7.35(m, 30H) MS: parent ion [M + H] $m/z = 1323(92)$, 1325(100).

3.3. Reaction of $CpFeMn(CO)_7$ with $Se{=}PPh_3$

A sample of $CpFeMn(CO)_7$ (34.0 mg, 0.091 mmol) was dissolved in 10 ml of MeCN in a 25 ml three-neck round-bottom flask equipped with a stir bar, gas inlet and gas outlet. To this solution was added 10.0 mg (0.090 mmol) of $Me_3NO{\cdot}2H_2O$, and the mixture was allowed to stir at r.t. for 1 h in the absence of light. Another equivalent of $Me_3NO{\cdot}2H_2O$ was added and stirred for additional 1 h. The solvent was removed in vacuo and the residues were dissolved in deoxygenated benzene (20 ml). To the resultant red solution was added 72.0 mg (two equivalents) of $SePPh_3$. The resulting dark brown solution was stirred at r.t. for 4 h. The volatiles were removed in vacuo. The residue was then dissolved in diethyl ether and filtered through a short column of silica gel. The solvent was removed again and the residue was separated by thin layer chromatography over silica gel by using a hexane–benzene–CH_2Cl_2 (2/1/1, v/v) solvent mixture as eluant. In order of elution, this yielded 2.3 mg (7% yield) of $CpFeMn_3(CO)_{15}(PPh_3)(\mu_3\text{-}Se)_2$ (**2**), 2.0 mg (4% yield) of $Cp_2Fe_2Mn_2(CO)_{10}(PPh_3)(\mu_3\text{-}Se)_2$ (**3**) and 5.2 mg (14% yield) of $Cp_2Fe_2Mn_2(CO)_{11}(\mu_3\text{-}Se)_2$ (**4**). Spectral data for **2**: IR ν_{CO} (cm^{-1} in CH_2Cl_2) 2075(m), 2041(w), 2010(vs), 1988(m, sh), 1965(w), 1933(m). ^{1}H-NMR (δ in CD_2Cl_2), 7.75–7.40 (m, 15H), 4.42 (s, 5H). MS: parent ion [M + H] $m/z = 1071(98)$, 1073(100). Spectral data for **3**: IR ν_{CO} (cm^{-1} in CH_2Cl_2) 2042(m), 2018(s, sh), 2001(vs), 1985(m, sh), 1948(m, sh), 1927(m). ^{1}H-NMR (δ in CD_2Cl_2), 7.60–7.35 (m, 15H), 4.91 (s, 5H), 4.39 (d, $^3J_{P-H} = 1.20$ Hz, 5H). MS: parent ion [M + H] $m/z =$ 1053(100), 1055(91). Spectral data for **4**: IR ν_{CO} (cm^{-1} in CH_2Cl_2) 2051(m), 2027(vs), 2003(s), 1992(s), 1933(m, br). ^{1}H-NMR (δ in C_6D_6), 3.97 (s, 10H). MS: parent ion [M + H] $m/z = 819(88)$, 821(100).

3.4. Crystallographic analyses

Red crystals of **1** and **3** were grown from a CH_2Cl_2–hexane solution at −17 °C. Red crystals of **2** were grown by slow evaporation of the solvent from a benzene–octane solution of the complex at 4 °C. The crystals used in data collections were glued onto the end of thin glass fibers. X-ray intensity data were measured at 293 K (150 K for **1**) on a Bruker SMART APEX CCD-based diffractometer using Mo–K_α radiation ($\lambda =$ 0.71073 Å). The unit cells were initially determined based on reflections collected from a set of three orthogonal scans. Crystal data, data collection parameters, and results of the analyses are listed in Table 1. The raw intensity data frames were integrated with the SAINT+ program which also applied corrections for Lorentz and polarization effects [15]. Final unit cell parameters are based on the least-squares refinement of all reflections with $I > 5(\sigma)I$ from the data sets. For each analysis an empirical absorption correction based on the multiple measurement of equivalent reflections was applied using the program SADABS [16].

Compound **1** crystallized in the monoclinic crystal system. Systematic absences were consistent with either of the space groups $C2/c$ or Cc. Intensity statistics indicated the centric space group $C2/c$, which was subsequently confirmed by successful solution and refinement of the structure. Compounds **2** and **3** both crystallized in the triclinic system. The space group $P\bar{1}$ was assumed and confirmed by successful solution and refinement of the structure. The structures were solved by a combination of direct methods and difference Fourier synthesis, and refined on F^2 by full-matrix least-squares using all data. All non-hydrogen atoms were refined with anisotropic displacement parameters. Hydrogen atom positions were calculated by assuming idealized geometries and refined by using the riding model. All calculations were performed with the

Table 1
Crystallographic data for compounds **1**, **2** and **3**

	1	**2**	**3**
Empirical formula	$Mn_4Se_2P_2O_{15}C_{51}H_{30}\cdot CH_2Cl_2$	$FeMn_3Se_2PO_{13}C_{36}H_{20}$	$Fe_2Mn_2Se_2PO_{10}C_{38}H_{25}$
Formula weight	1405.28	1070.08	1052.05
Crystal system	Monoclinic	Triclinic	Triclinic
Lattice parameters			
a (Å)	19.1623(8)	9.7947(14)	9.4979(13)
b (Å)	10.5405(4)	11.4197(16)	12.8475(17)
c (Å)	28.0092(11)	17.644(3)	17.839(2)
α (°)	90	87.057(3)	70.074(3)
β (°)	103.459(1)	83.147(4)	75.849(3)
γ (°)	90	89.429(4)	77.797(3)
V (Å^3)	5501.9(4)	1956.8(5)	1964.7(5)
Space group	$C2/c$	$P\bar{1}$	$P\bar{1}$
Z value	4	2	2
ρ_{calc} (g cm^{-3})	1.697	1.816	1.778
μ (Mo–K$_\alpha$) (mm^{-1})	2.44	3.27	3.30
Temperature (K)	150	296	296
$2\Theta_{max}$ (°)	50.10	52.08	48.82
Number of observations [$I > 2\sigma(I)$]	4036	5598	3654
Number of parameters	413	505	496
Goodness-of-fit	1.000	1.111	0.982
Maximum shift in final cycle	0.002	0.000	0.000
Residuals*: R_1; wR_2	0.0338; 0.0822	0.0588; 0.1266	0.0578; 0.1164
Transmission coefficient max/min	0.831/0.668	1/0.805	1/0.652
Largest peak in final differential Fourier (e Å^{-3})	0.96	0.81	1.03

* $R_1 = \Sigma(||F_{obs}|-|F_{calc}||)/\Sigma|F_{obs}|$. $wR_2 = \{\Sigma[w(F^2_{obs}-F^2_{calc})^2/\Sigma[w(F^2_{obs})^2]\}^{1/2}$; $w = 1/\sigma^2(F^2_{obs})$. GOF $= [\Sigma_{hkl}(w(|F^2_{obs}|-|F^2_{calc}|))^2/(n_{data}-n_{vari})]^{1/2}$.

SHELXTL software package by using neutral atom scattering factors [16].

4. Supplementary information

CIF files for the structural analyses have been deposited with the Cambridge Crystallographic Data Center CCDC 211383–211385 for compounds for **1**–**3**, respectively. Copies of this information can be obtained free of charge from The Director, CCDC, 12 Union Road, Cambridge CB2 1EZ, UK (Fax: +44-1223-336033; e-mail: deposit@ccdc.cam.ac.uk or www: http://www.ccdc.cam.ac.uk).

Acknowledgements

This research was supported by a grant from the National Science Foundation, CHE-9909017.

Table 2
Selected intramolecular distances and angles for $Mn_4(CO)_{15}(PPh_3)_2(\mu_3\text{-}Se)_2$ (**1**) [a]

Atom	Atom	Distance (Å)	Atom	Atom	Distance (Å)
(*a*) *Distances*					
Mn(1)	Mn(1′)	2.6771(9)	Mn(1)	Se(1′)	2.4643(5)
Mn(1)	Se(1)	2.4546(5)	Mn(2)	Se(1)	2.5277(5)

Atom	Atom	Atom	Angle (°)	Atom	Atom	Atom	Angle (°)
(*b*) *Angles*							
Se(1)	Mn(1)	Se(1′)	75.772(18)	Mn(1′)	Se(1)	Mn(2)	120.826(19)
Se(1)	Mn(1)	Mn(1′)	57.201(16)	O(10)	C(10)	Mn(1)	140.01(9)
Se(1′)	Mn(1)	Mn(1′)	56.852(16)	O(10)	C(10)	Mn(1′)	140.01(9)
Mn(1)	Se(1)	Mn(1′)	65.95(2)	Mn(1)	C(10)	Mn(1′)	79.97(18)
Mn(1)	Se(1)	Mn(2)	119.782(19)				

[a] Estimated standard deviations in the least significant figure are given in parentheses.

Table 3
Selected intramolecular distances and angles for $CpFeMn_3(CO)_{13}(PPh_3)(\mu_3\text{-}Se)_2$ (**2**) and $Cp_2Fe_2Mn_2(CO)_{10}(PPh_3)(\mu_3\text{-}Se)_2$ (3) [a]

2			**3**		
Atom	Atom	Distance (Å)	Atom	Atom	Distance (Å)
(*a*) *Distances*					
Mn(1)	Mn(2)	2.6771(14)	Mn(1)	Mn(2)	2.6861(18)
Mn(1)	Se(1)	2.4612(11)	Mn(1)	Se(1)	2.4921(16)
Mn(1)	Se(2)	2.4587(12)	Mn(1)	Se(2)	2.4896(17)
Mn(2)	Se(1)	2.4755(11)	Mn(2)	Se(1)	2.4516(16)
Mn(2)	Se(2)	2.4596(12)	Mn(2)	Se(2)	2.4393(17)
Mn(3)	Se(1)	2.5387(10)	Fe(1)	Se(1)	2.4215(15)
Fe(1)	Se(2)	2.4255(11)	Fe(2)	Se(2)	2.4249(17)
Mn(1)	C(13)	2.080(8)	Mn(1)	C(13)	2.006(11)
Mn(2)	C(13)	2.079(8)	Mn(2)	C(13)	2.128(11)

2				**3**			
Atom	Atom	Atom	Angle (°)	Atom	Atom	Atom	Angle (°)
(*b*) *Angles*							
Se(2)	Mn(1)	Se(1)	75.06(3)	Se(2)	Mn(1)	Se(1)	74.92(5)
Se(2)	Mn(1)	Mn(2)	57.04(3)	Se(2)	Mn(1)	Mn(2)	56.08(5)
Se(1)	Mn(1)	Mn(2)	57.42(3)	Se(1)	Mn(1)	Mn(2)	56.37(4)
Se(2)	Mn(2)	Se(1)	74.78(3)	Se(2)	Mn(2)	Se(1)	76.56(5)
Se(2)	Mn(2)	Mn(1)	57.01(3)	Se(2)	Mn(2)	Mn(1)	57.88(5)
Se(1)	Mn(2)	Mn(1)	56.90(3)	Se(1)	Mn(2)	Mn(1)	57.82(4)
Mn(1)	Se(1)	Mn(2)	65.68(4)	Fe(1)	Se(1)	Mn(2)	115.03(6)
Mn(1)	Se(1)	Mn(3)	125.76(4)	Fe(1)	Se(1)	Mn(1)	128.46(6)
Mn(2)	Se(1)	Mn(3)	117.71(4)	Mn(2)	Se(1)	Mn(1)	65.82(5)
Fe(1)	Se(2)	Mn(1)	120.93(4)	Fe(2)	Se(2)	Mn(2)	116.53(6)
Fe(1)	Se(2)	Mn(2)	119.55(4)	Fe(2)	Se(2)	Mn(1)	122.79(6)
Mn(1)	Se(2)	Mn(2)	65.95(4)	Mn(2)	Se(2)	Mn(1)	66.04(5)
Mn(2)	C(13)	Mn(1)	80.1(3)	Mn(1)	C(13)	Mn(2)	81.0(4)

[a] Estimated standard deviations in the least significant figure are given in parentheses.

References

[1] (a) M. Hidai, S. Kuwata, Y. Mizobe, Acc Chem. Res. 33 (2000) 46;
(b) M. Oakzaki, M. Yuki, K. Kuge, H. Ogino, Coord. Chem. Rev. 198 (2000) 367;
(c) L.C. Roof, J.W. Kolis, Chem. Rev. 93 (1993) 1037;
(d) P. Mathur, Adv. Organomet. Chem. 41 (1997) 243.

[2] (a) S.-W. Audi Fong, T.S.A. Hor, J. Chem. Soc. Dalton Trans. (1999) 639;
(b) T. Shibihara, Coord. Chem. Rev. 123 (1993) 73;
(c) K.H. Whitmire, J. Coord. Chem. 17 (1998) 95;
(d) R.D. Adams, M. Tasi, J. Cluster Sci. 1 (1990) 249;
(e) R.D. Adams, Polyhedron 4 (1985) 2003.

[3] (a) S. Dehnen, A. Eichhofer, D. Fenske, Eur. J. Inorg. Chem. (2002) 279;
(b) P. Braunstein, C. Graiff, C. Massera, G. Predieri, J. Rose, A. Tiripicchio, Inorg. Chem. 41 (2002) 1372.

[4] R.D. Adams, O.S. Kwon, Inorg. Chem., in press.

[5] (a) S.M. Stuzynski, Y.U. Kwon, M.L. Steugerward, J. Organomet. Chem. 449 (1993) 167;
(b) W. Imhof, G. Huttner, J. Organomet. Chem. 448 (1993) 247;
(c) P. Baistrochi, M. Careri, D. Cauzzi, C. Graiff, M. Lanfranchi, P. Manini, G. Predieri, A. Tiripicchio, Inorg. Chim. Acta 252 (1996) 367;
(d) D. Cauzzi, C. Graiff, M. Lanfranchi, G. Predieri, A. Tiripicchio, J. Chem. Soc. Dalton Trans. (1995) 2321.

[6] (a) R.D. Adams, O.S. Kwon, M.D. Smith, Inorg. Chem. 40 (2001) 5322;
(b) R.D. Adams, O.S. Kwon, M.D. Smith, Inorg. Chem. 41 (2002) 6281.

[7] M. Martin, B. Rees, A. Mitschler, Acta Crystallogr. Sect. B 38 (1982) 6.

[8] M.R. Churchill, K.N. Amoh, H.J. Wasserman, Inorg. Chem. 20 (1981) 1609.

[9] S.C. O'Neal, W.T. Pennington, J.W. Kolis, Inorg. Chem. 29 (1990) 3134.

[10] S. Jäger, P.G. Jones, J. Laube, C. Thöne, Z. Anorg. Allg. Chem. 625 (1999) 352.

[11a] C.F. Campana, F.Y.K. Lo, L.F. Dahl, Inorg. Chem. 18 (1979) 3060.

[11b] P. Baistrocchi, M. Careir, D. Cauzzi, C. Graiff, M. Lanfrachi, P. Manini, G. Predieri, A. Tiripicchio, Inorg. Chim. Acta 252 (1996) 367.

[12] P. Johnston, G.J. Hutchings, L. Denner, J.C.S. Boeyens, N.J. Coville, Organometallics 6 (1987) 1292.

[13] V. Koelle, J. Organomet. Chem. 155 (1978) 53.

[14] R.K. Bhardwaj, S. Davidson, Terahedron 43 (1987) 4473.

[15] SAINT+ Version 6.02a, Bruker Analytical X-ray System, Inc., Madison, WI, USA, 1998.

[16] G.M. Sheldrick, SHELXTL Version 5.1, Bruker Analytical X-ray Systems, Inc, Madison, WI, USA, 1997.